Optimal parameter estimation for methyl methacrylate polymerization

V. Ravi Kumar and Santosh K. Gupta*
Department of Chemical Engineering, Indian Institute of Technology, Kanpur 208016, India
(Received 3 May 1990; revised 24 September 1990; accepted 14 December 1990)

Several different sets of correlations have been proposed for methyl methacrylate polymerization for the three parameters, θ_p, θ_t and A, characterizing the gel and glass effects in the model of Chiu *et al.* It is found that these correlations do not explain isothermal batch reactor data particularly well. An optimal parameter estimation technique has been used to obtain new correlations, and it is found that the agreement between calculation and experiment improves significantly. The technique is quite general, and as a further illustration it has been used to develop correlations for the gel and glass effects for polystyrene, at temperatures which are sufficiently low that thermal initiation is absent.

(Keywords: optimization; polymerization; methyl methacrylate)

INTRODUCTION

In the last few years a considerable amount of literature has become available on the modelling of the molecular mechanisms underlying the gel or Trommsdorff effect in chain polymerization systems[1-4]. The gel effect arises because of a continuous decrease in the termination rate constant k_t ($= k_{tc} + k_{td}$, *Table 1*), as the monomer conversion increases. This is associated with an increase in the viscosity of the reaction mass. This phenomenon leads to higher monomer conversions than predicted by models using constant values for the rate constants, determined from low conversion data. In addition to this, a glass effect is also exhibited at conversions close to unity. The propagation rate constant, k_p, starts decreasing when the reaction mass crosses over to below the glass transition point. This phenomenon leads to the polymerization stopping short of complete conversion.

In the past few decades, several researchers have tried to explain experimental data by extending the kinetic model to account for the gel and glass effects. These have been discussed in detail and reviewed by several authors[1,5-10]. Friis and Hamielec[8] and Ross and Laurence[9], for example, have used simple empirical correlations to describe the polymerization kinetics. They have proposed correlations for the apparent rate constants in terms of several system parameters, such as conversion, temperature and free volume. They have assumed a small gel effect initially but a much stronger effect at lower free volumes or higher conversions. Cardenas and O'Driscoll[10], on the other hand, have divided the polymer species into two populations, one having a degree of polymerization (DP) below a critical value and the other having a DP above it. The k_t for the latter was taken as a parameter to be obtained by curve-fitting experimental data. These three groups and most of the other earlier workers have introduced diffusional restrictions on the rate constants at some break point.

Recently, Chiu *et al.*[1] proposed a phenomenological model using a molecular viewpoint. In their model, diffusional limitation was considered to be an integral part of the chain termination process. The effects of temperature, concentration and molecular weight on the relative importance of reaction *versus* diffusion were accounted for, and it was found that experimental data on poly(methyl methacrylate) (PMMA) could be explained fairly well. This model offers an additional benefit in that there are no discontinuities present, and so is suitable for use in engineering studies involving simulation, optimization, control, parametric sensitivity[11], etc., of such systems. Sharma and Soane[12] have recently extended this model to more complex copolymerization systems, while Achilias and Kiparissides[5] have proposed a methodology for predicting the values of the various parameters fundamentally.

It is well recognized and documented[1,3] that all these models for the gel and glass effects are about equally successful in explaining experimental rate data under a variety of conditions, even though they offer varying amounts of insight into the physical processes involved. This probably explains the recent rise in popularity of the simple model of Chiu *et al.*[1]. Unfortunately, there is

Table 1 Kinetic scheme for chain polymerization

$I \xrightarrow{k_d} 2R^*$	Initiation
$R^* + M \xrightarrow{k_i} P_1$	
$P_n + M \xrightarrow{k_p} P_{n+1}$	Propagation
$P_n + M \xrightarrow{k_{tr}} D_n + P_1$	Chain transfer to monomer
$P_n + P_m \xrightarrow{k_{td}} D_n + D_m$	Termination by disproportionation
$P_n + P_m \xrightarrow{k_{tc}} D_{n+m}$	Termination by combination

* To whom correspondence should be addressed

0032-3861/91/173233-11

some confusion regarding the values of the parameters to be used in this model. The correlations suggested by Baillagou and Soong[14,15] for two parameters, θ_t and θ_p, do not agree with the experimental data[16,17] on PMMA. Similarly, the correlations for θ_t and θ_p developed by Louie *et al.*[18] on the same system differ from those of Baillagou and Soong, even though both emanate from the same laboratory. The same applies to the values reported by Carratt *et al.*[19]. In our earlier work on the parametric sensitivity of tubular PMMA reactors[11], we have suggested our own values for these parameters, obtained using a trial and error procedure. The technique is suspect, particularly since more than a single parameter is present, and there is a need to develop a systematic procedure to obtain the values of the parameters.

In this study, we focus attention on obtaining the best-fit values for parameters in the multi-parameter model of Chiu *et al.*[1] using an optimization technique which minimizes the mean square error between experimental and predicted values. We present results for PMMA using isothermal batch reactor data[16,17]. Even though the results are specific to PMMA the approach is general, and can be used not only to obtain optimal parameter values for the gel effect in other chain polymerization systems [some results on polystyrene (PS) are also included to illustrate this], but also for obtaining optimal parameters for any system described by non-linear, coupled ordinary (or even partial) differential equations.

FORMULATION

The kinetic mechanism of free radical polymerization considered in this work is summarized in *Table 1*. This is typical of PMMA as well as several other chain polymerization systems. There are four major reactions: initiation, propagation, chain transfer to monomer and termination, both by combination and disproportionation. In some systems, reactions like thermal initiation of monomer could occur (as for PS at high temperatures), but these are not included here (although they could be incorporated quite easily).

In the initiation step, homolytic dissociation of an initiator molecule yields a pair of radicals, R*, to which monomer molecules add on to produce the chain initiating species P_1. Successive addition of a large number of monomer molecules occurs by the propagation reaction to give high chain length radicals, P_n. The bimolecular reaction between two growing radicals leads to termination, producing dead polymer molecules, D_n. The growing radicals could either combine with each other, giving a single, longer dead polymer molecule (combination), or could lead to two dead polymer molecules (disproportionation) having the same chain lengths as the radicals. Termination of a growing polymer radical could also take place by the transfer of the radical to a monomer molecule (chain transfer).

As polymerization progresses the termination rate constants, k_{tc} and k_{td}, and the propagation rate constant, k_p, decrease due to diffusional limitations. The apparent rate constants are, therefore, functions of those physical properties of the system which determine the rate of diffusion of the long radicals. One such model has been suggested by Chiu *et al.*[1] and is summarized in *Table 2*, along with the mass balance equations for isothermal batch polymerizations. The rate constants, k_p and k_t, are written in terms of the values, k_{po} and k_{to}, in the absence of the gel effect (indicated by subscript o). In writing these equations, it is assumed that the rate constant for chain transfer, k_{tr}, decreases, in a manner similar to that predicted for k_p:

$$\frac{k_{tr}}{k_{tro}} = \frac{k_p}{k_{po}} \tag{1}$$

This is a reasonable approximation[11] since these two reactions involve the same kinds of diffusional mechanisms, i.e. monomer molecules diffusing towards a growing chain radical.

The non-linear coupled ordinary differential equations (ODEs) in *Table 2* are integrated using a double-precision Gear's package (NAG library subroutine D02EBF, using a tolerance of 10^{-12}) to give the characteristics of the reaction mass as a function of time, for a given temperature, T, and initiator concentration, I_0, in the feed. The gel and glass effect parameters, θ_p, θ_t and A (for any temperature and I_0), are best obtained by curve-fitting and are estimated optimally in this study, using the Box complex method[20-22] (*Table 3*), so as to minimize the least square error between experimental data and model predictions. The error, E, is taken as:

$$E(\theta_p, \theta_t, A) = \frac{1}{2N}\sum_{i=1}^{N}\left\{\left[\frac{|x_i^{exp} - x_i^{th}|}{x_i^{exp}}\right] + \left[\frac{|M_{n,i}^{exp} - M_{n,i}^{th}|}{M_{n,i}^{exp}}\right]\right\} \tag{2}$$

where the superscripts exp and th indicate the experimental and theoretical values, respectively, and N is the number of data points for monomer conversion, x_i, and the number average molecular weight, $M_{n,i}$ (at time $t = t_i$). All the other kinetic parameters used for simulation are listed in *Table 4* for PMMA[1,11,12] (*Table 5* gives similar information for PS[12,23-26]). It may be added that the choice of equation (2) as an error definition is somewhat non-unique. In fact, it can be argued that this choice suffers from the disadvantage that more weightage is given to points at low values of x_i^{exp} (below ~ 0.5) than to data at higher conversions. But, it may be noted that the gel effect equations start contributing only at values of x_i above ~ 0.5, in which range we are fitting the three parameters, θ_p, θ_t and A.

For this optimization work, we adopt the Box complex method[20-22] with constraints on the values of the parameters, θ_p, θ_t and A (*Table 3*). The initial 'complex' is generated using four points (vertices) in the three-dimensional (θ_p, θ_t, A) space using a set of prespecified numbers, r_{ij}. This complex rolls around and contracts to near the minimum of E. The advantage of this technique is that it does not require any derivatives.

A computer program using the Box complex technique was produced and tested on a sample problem[22]:

$$\begin{aligned} &\text{Maximize} && F(X) = X_1\ X_2\ X_3 && \text{(a)} \\ &\text{subject to:} && 72 - X_1 - 2X_2 - 2X_3 \geqslant 0 && \text{(b)} \\ & && 0 \leqslant X_1 \leqslant 20 && \text{(c)} \\ & && 0 \leqslant X_2 \leqslant 11 && \text{(d)} \\ & && 0 \leqslant X_3 \leqslant 42 && \text{(e)} \end{aligned} \tag{3}$$

Table 2 Mass balance and gel and glass effect equations

$$\frac{dx}{dt} = \frac{(1 + \varepsilon x)}{M_0} K$$

$$K = [\varepsilon_1 k_p R^* + (k_p + k_{tr})\lambda_0] M$$

$$M = M_0(1 - x)/(1 + \varepsilon x)$$

$$\frac{dI}{dt} = -k_d I - \frac{\varepsilon K I}{M_0}$$

$$\frac{dR^*}{dt} = 2fk_d I - \varepsilon_1 k_p M R^* - \frac{\varepsilon K R^*}{M_0}$$

$$\frac{d\lambda_0}{dt} = \varepsilon_1 k_p M R^* - (k_{td} + k_{tc})\lambda_0^2 - \frac{\varepsilon K \lambda_0}{M_0}$$

$$\frac{d\lambda_1}{dt} = \varepsilon_1 k_p W M R^* + W k_p M \lambda_0 - (k_{td} + k_{tc})\lambda_0\lambda_1 + k_{tr} M(W\lambda_0 - \lambda_1) - \frac{\varepsilon K \lambda_1}{M_0}$$

$$\frac{d\lambda_2}{dt} = \varepsilon_1 k_p W^2 M R^* - (k_{tc} + k_{td})\lambda_0\lambda_2 + k_p M W(2\lambda_1 + W\lambda_0) + k_{tr} M(W^2\lambda_0 - \lambda_2) - \frac{\varepsilon K \lambda_2}{M_0}$$

$$\frac{d\mu_0}{dt} = (k_{td} + 0.5k_{tc})\lambda_0^2 + k_{tr} M \lambda_0 - \frac{\varepsilon K \mu_0}{M_0}$$

$$\frac{d\mu_1}{dt} = (k_{td} + k_{tc})\lambda_0\lambda_1 + k_{tr}\lambda_1 M - \frac{\varepsilon K \mu_1}{M_0}$$

$$\frac{d\mu_2}{dt} = (k_{td} + k_{tc})\lambda_0\lambda_2 + k_{tc}\lambda_1^2 + k_{tr}\lambda_2 M - \frac{\varepsilon K \mu_2}{M_0}$$

Constitutive equations for the gel and glass effects[1]

$$\frac{1}{k_t} = \frac{1}{k_{to}} + \theta_t(T, I_0) - \exp\left[\frac{2.303\phi_m}{A(T) + B\phi_m}\right]$$

$$\frac{1}{k_p} = \frac{1}{k_{po}} + \theta_p(T) - \exp\left[\frac{2.303\phi_m}{A(T) - B\phi_m}\right]$$

$$\phi_m = \frac{1 - x}{1 + \varepsilon x}$$

$$\theta_p = \theta_p^0 \exp\left(\frac{E_{\theta p}}{RT}\right)$$

$$\theta_t = \frac{\theta_t^0}{I_0} \exp\left(\frac{E_{\theta t}}{RT}\right)$$

$$A(T) = C_1 - C_2(T - T_{gp})^2$$

The optimal solution is known for this problem to be $X = [20, 11, 15]^T$, at which point F is 3300. Values of $\alpha = 1.3$, $\beta = 0.1$ and $\gamma = 5$ (*Table 3*) were used and the initial value of X was taken as $[10, 10, 10]^T$. The other three points on the initial complex were generated by the computer. The maximum objective function calculated by the routine was 3299.8132 with $X = [19.9986, 10.999, 15.002]^T$, which is observed to be fairly close to the optimum. The routine took 140 iterations and 1.75 s of CPU time on a DEC-1090 system. Fewer iterations are required for higher tolerances (β).

In the present study, the objective function used is

$$\text{Max } F(\theta_p, \theta_t, A) = -E(\theta_p, \theta_t, A) \qquad (4)$$

with E defined by equation (2) (maximization of F is equivalent to minimization of E). A single iteration in the Box complex technique requires the solution of a set of seven stiff ordinary differential equations (*Table 2*) from time $t = 0$ to some large value (so that the last data point is incorporated) for one set of values for θ_p, θ_t and A, and then computing the error, E, using the computed and experimental values of x_i and $M_{n,i}$ at the different values of time, t_i. In the case of PMMA, a single iteration requires 2 min of CPU time on the DEC-1090 system, the large time being a consequence of the stiffness of the mass balance equations. Over 30 iterations are required to obtain the parameters for one set of T and I_0, provided the optimum values lie in the given ranges specified for the three parameters. Several techniques were tried to reduce the computational effort. The technique finally adopted is interactive. An initial set of four points [vertices of the complex, X_i (= X_1, X_2, X_3)$_i$, where $(X_j)_i$ represents the jth coordinate of the ith point in the three-dimensional parameter space] is chosen using the equations in *Table 3*. Then the Box complex program is run for three iterations to give four final points, $X_{1,f}$, $X_{2,f}$, $X_{3,f}$ and $X_{4,f}$ along with the values of ($-E$) at these points (the tolerance condition is not necessarily met). The best of these four points, say X_f^*, is selected, and a new set of four points (with a smaller range around X_f^*),

Table 3 Simplified Box complex[a] technique[20-22]

Objective function:

Maximize $F(X_1, X_2, \ldots, X_N)$

Constraints (feasible region):

$G_i \leqslant X_i \leqslant H_i, \quad i = 1, 2, \ldots, N$

Procedure:

(1) Generate 'complex':

input $X_1 = [X_1, X_2, \ldots, X_N]_1^T$

$(X_i)_j = G_i + r_{ij}(H_i - G_i), \quad i = 1, 2, 3, \ldots, N$

$j = 2, 3, \ldots, N + 1$

(2) Evaluate $F(X_j), \quad j = 1, 2, \ldots, N + 1$

(3) Select kth point for which $F(X_k)$ is minimum

(4) Replace kth worst point:

$X_k^{new} = \alpha(X_m - X_k) + X_m$

where $X_m = (1/N) \sum_{j=1}^{N+1} (X_j - X_k)$

(5) Check constraints:

$(X_i^{new})_k = (H_i - \delta)$

or $(G_i + \delta); \quad i = 1, 2, \ldots, N$

if constraint violated

(6) Evaluate $F(X_k^{new})$ and check if X_k^{new} is minimum point again

if yes: $X_k^{new} = (X_k^{new} + X_m)/2.0$

Repeat step (5)

if no: this completes one iteration; go to step (3)

(7) Stop when

$|F(X_i) - F(X_j)| \leqslant \beta, \quad i, j = 1, 2, \ldots, N$

$i \neq j$

for γ consecutive iterations

[a]Only explicit constraints considered

Table 4 Parameters used for PMMA[1,11,12]

f	0.58 (AIBN)
ρ_m (kg m^{-3})	$966.5 - 1.1[T(K) - 273.1]$
ρ_p (kg m^{-3})	1200
ε	$-\{0.1946 + 0.916 \times 10^{-3}[T(K) - 273.1]\}$
T_{gP} (K)	387.1
k_d^o (s^{-1})	1.053×10^{15}
k_{po}^o (m^3 mol^{-1} s^{-1})	4.917×10^2
k_{tdo}^o (m^3 mol^{-1} s^{-1})	9.8×10^4
k_{tc}^o	0.0
k_{tr}^o	0.0
E_d (kJ mol^{-1})	128.45
E_P (kJ mol^{-1})	18.22
E_{td} (kJ mol^{-1})	2.937
B	0.03
ε_1	1.0

Superscripts o indicate that these are the frequency factors in the corresponding Arrhenius equation (with E_d, E_P, E_{td}, etc., being the activation energies)

is generated from the algorithm. The procedure is repeated several times till the tolerance limit is met (the number of iterations being increased near the end). This interactive procedure leads to a lower total CPU time than required using some other approaches. In fact, in the last stages even the values of r_{ij} can be fine-tuned to attain faster convergence.

RESULTS AND DISCUSSION

We first present computational results for PMMA, using the values of θ_p, θ_t and A as given by four different research groups (cases a[14,15], b[18], c[19] and d[11], *Table 6*). *Figures 1* and *2* show the conversion histories at two different temperatures (50°C, 90°C) for $I_0 = 15.48$ mol m^{-3}. Experimental data[16,17] are also shown in these figures. The agreement between computed and experimental results is observed to be quite poor. Similar conclusions are found for other temperatures and initiator concentrations. In fact, this was the reason for this study.

The optimal parameter estimation package is then used (with values given in *Table 7*) for PMMA under different conditions (T, I_0 values) for which experimental data (from one research group[1,16,17]) are available. It is observed that several experimental data points are available in the low conversion region, i.e. before the gel effect region, but in the more important zone where this phenomenon becomes significant, the number of data points is far smaller. We drew smooth curves passing

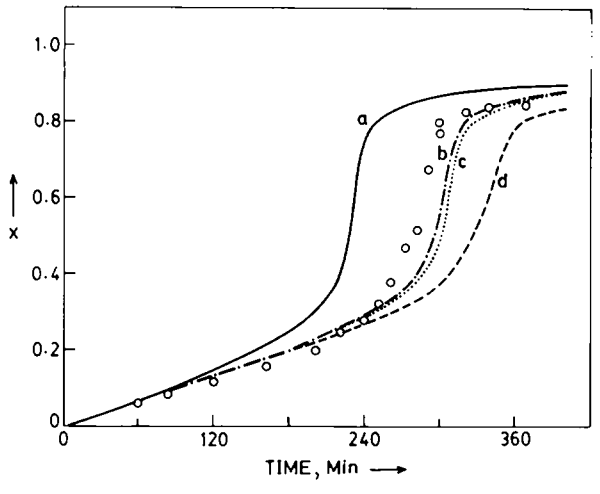

Figure 1 Comparison of simulated results on batch reactor conversion and experimental data on PMMA at 50°C ($I_0 = 15.48$ mol m^{-3}) using the parameters from the literature. See *Table 6* for correlations used

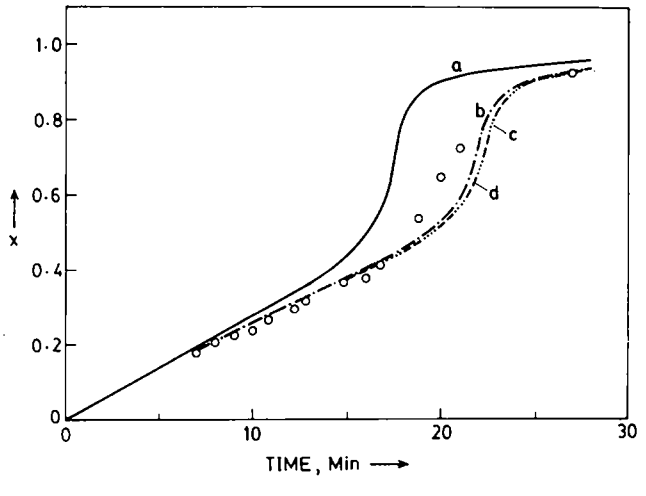

Figure 2 Comparison of simulated results and experimental data on PMMA at 90°C ($I_0 = 15.48$ mol m^{-3}) using parameters from the literature. Notation same as in *Figure 1*. Curves c and d are indistinguishable

Table 5 Parameters used for PS[12,23-26]

f	$-12.342396 + 9577.287/T(\mathrm{K}) - 1743120.6/[T(\mathrm{K})]^2$	(this work)
ρ_m (kg m^{-3})	$924 - 0.918[T(\mathrm{K}) - 273.16]$	(23)
ρ_p (kg m^{-3})	$1084.8 - 0.685[T(\mathrm{K}) - 273.16]$	(23)
ε	$[\rho_m - \rho_p]/\rho_p$	
T_{gp} (K)	373.16	(25)
k_d^o (s^{-1})	2.67×10^{15}	(25)
k_{po}^o (m^3 mol^{-1} s^{-1})	1.051×10^4	(24)
k_{tdo}	0.0	
k_{tco}^o (m^3 mol^{-1} s^{-1})	1.26×10^6	(24)
k_{tro}^o (m^3 mol^{-1} s^{-1})	2.31×10^3	(26)
E_d (kJ mol^{-1})	130.3	(25)
E_p (kJ mol^{-1})	29.58	(24)
E_{tc} (kJ mol^{-1})	7.04	(24)
E_{tr} (kJ mol^{-1})	52.75	(26)
B	0.02	(12)
ε_1	1.0	

References indicated in parentheses

Table 6 Correlations for gel and glass effect parameters for PMMA[11,14,15,18,19]

Case	Ref.	$10^{14}\theta_p^o$ (s)	$10^{17}\theta_t^o$ (s mol m^{-3})	$E_{\theta p}$ (kJ mol^{-1})	$E_{\theta t}$ (kJ mol^{-1})	C_1	$10^6 C_2$ (K^{-2})
a	14, 15	2.3723	1.3473	117.3	145.0	0.168	8.21
b	18	3.2888	0.6812	116.4	145.0	0.168	8.21
c	19	3.2880	0.6840	116.5	144.8	0.168	8.21
d	11	3.2888	0.6932	118.1	144.1	0.168	8.21
e	This work	399.822	0.28883	102.451	148.924	0.15998	7.812

$\theta_p = \theta_p^o \exp(E_{\theta p}/RT)$

$\theta_t = \dfrac{\theta_t^o}{I_0} \exp(E_{\theta t}/RT)$ with I_0 in mol m^{-3}

$B = 0.03$

Table 7 Parameters used in the Box complex method[21]

$N = 3$
$\alpha = 1.3$
$\beta = 0.1 \cdot N_{used}$
$\gamma = 5$
$\delta = 10^{-5}$

Prechosen numbers:

$r_{21} = 0.025$	$r_{22} = 0.35$	$r_{23} = 0.75$
$r_{31} = 0.35$	$r_{32} = 0.75$	$r_{33} = 0.025$
$r_{41} = 0.75$	$r_{42} = 0.025$	$r_{43} = 0.35$

through the experimental points and then took a number, N_{used}, of equally spaced points (though slightly artificial) from these curves. Using this technique we could give more emphasis to the gel effect region as compared to the low conversion region. The values of N_{used} for different runs are listed in *Table 8*, along with the actual number, N_{exp}, of experimental data points. It should be noted that several other ways could have been devised to increase the emphasis on the fewer experimental data points in the gel effect region, each as good as the other. The

Table 8 Error predictions using optimal parameters for PMMA

Temp. (°C)	I_0 (mol m^{-3})	N_{exp} (no. of exp. points)	N_{used} (no. of data points)	E (using optimal parameters)	E (using regression correlations)
50	15.48	17	13	0.1167	0.1254
	20.18	15	10	0.05711	0.0590
	25.8	27	10	0.0478	0.0613
70	15.48	17	15	0.0561	0.0745
	25.8	18	13	0.0537	0.0644
90	15.48	20	14	0.0528	0.071
	25.8	18	12	0.0716	0.0757

Table 9 Optimal parameters for PMMA[a]

Temp. (°C)	I_0 (mol m^{-3})	$10^{-5}\theta_p$ (s)	$10^{-5}\theta_t$ (s)	A
50	25.8	1.8331	1.3552	0.12784
	20.18	1.8331	1.7326	0.127814
	15.48	1.8331	2.2586	0.1278
70	25.8	0.1146	0.04080	0.1455
	15.48	0.1162	0.07207	0.1456
90	25.8	0.02493	0.003147	0.15454
	15.48	0.02433	0.005150	0.15556

[a]Correlations (regression):

$\theta_p(s) = 3.9982 \times 10^{-12} \exp(102.451/RT)$

$\theta_t(s) = \dfrac{2.8883 \times 10^{-18}}{I_0} \exp(148.924/RT)$

$A = 0.159977 - 7.811953 \times 10^{-6}[T(K) - 387.1]^2$

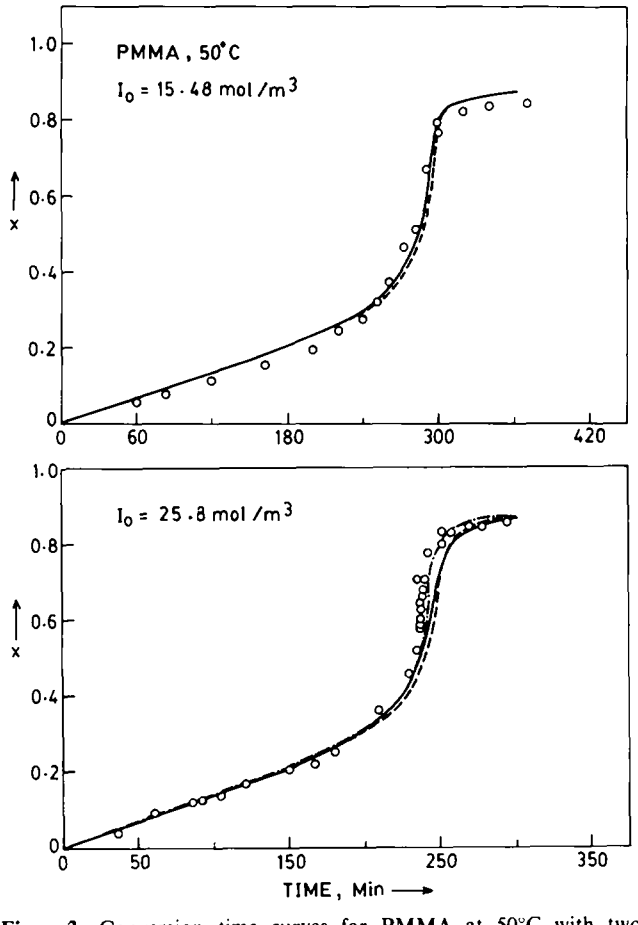

Figure 3 Conversion–time curves for PMMA at 50°C with two initiator loadings: (— · — · —) using individual optimal parameters; (---) using regression correlations; (— · —) with k_{tc} and k_{tr}. Experimental data[16,17] indicated by circles

parameters θ_p, θ_t and A differ considerably in magnitude. These are scaled appropriately so that the parameters, X_1, X_2 and X_3 used in the program vary from ~0 to 1. Scaling ensures faster convergence to the optimum.

Table 9 presents the optimal values of the parameters for different values of temperature and initiator concentration. The corresponding errors, E, at the optimal condition are listed in *Table 8*. *Figures 3–6* show the conversion histories predicted using the optimal parameters. The agreement between the experimental results and the theoretical predictions is seen to be superior to that shown in *Figures 1* and *2*. The corresponding plots for the number average molecular weights, M_n, *versus* monomer conversion, x, are shown in *Figures 7* and *8*. Again, the agreement between experimental and theoretical predictions is satisfactory. Experimental data for the weight average molecular weight, M_w, are not used in the computation of the optimal parameters for two reasons. First, the data for M_w show much more scatter than shown by M_n data, and it is better not to include it in the objective function, E. Second, the model of Chiu *et al.*[1] does not give a very good fit to M_w data (as observed by those workers) and so it is better not to influence the gel effect parameters by adding terms for M_w in E. *Figures 9* and *10* show the predictions of M_w together with experimental data.

Chiu *et al.*[1] have suggested that θ_p and θ_t can be fitted using the following equations:

$$\theta_p = \theta_p^\circ \exp(E_{\theta p}/RT) \quad \text{(a)}$$

$$\theta_t = \frac{\theta_t^\circ}{I_0} \exp(E_{\theta t}/RT) \quad \text{(b)} \qquad (5)$$

$$A = C_1 - C_2(T - T_{gp})^2 \quad \text{(c)}$$

Figures 11 and *12* show plots of $\ln(1/\theta_t I_0)$ and $\ln(1/\theta_p)$ *versus* $10^3/T$ and of A *versus* $(T - T_{gp})^2$. A regression analysis is carried out on the optimal parameters obtained at different conditions, to give values of θ_p°, $E_{\theta p}$, θ_t°, $E_{\theta t}$, C_1 and C_2. The correlations obtained are given in *Table 9*. (These are also shown as straight lines in *Figures 11* and *12*.) A comparison of these correlations with the four sets of earlier correlations (based on the same model) is shown in *Table 6*. Substantial differences are observed from the earlier correlations. *Figures 3–10* also show the computed results using these regression correlations along with the predictions using the individual best-fit parameters. It is found that the use of these correlations is justified (the slightly larger deviations at 70°C between results obtained using correlations as opposed to those from best-fit parameter values are also reflected in *Figure 11* for the θ_p point at this temperature). These correlations are recommended for use in future studies on the reaction engineering of PMMA systems.

It may be mentioned at this point that Rawlings and

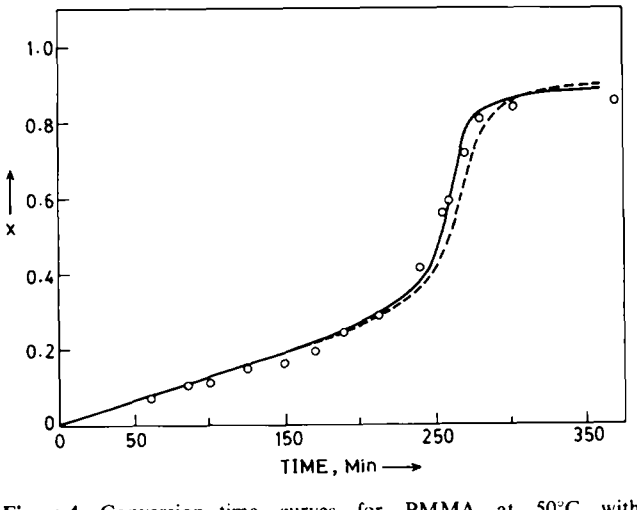

Figure 4 Conversion–time curves for PMMA at 50°C with I_0 = 20.18 mol m^{-3}. Notation same as in *Figure 3*

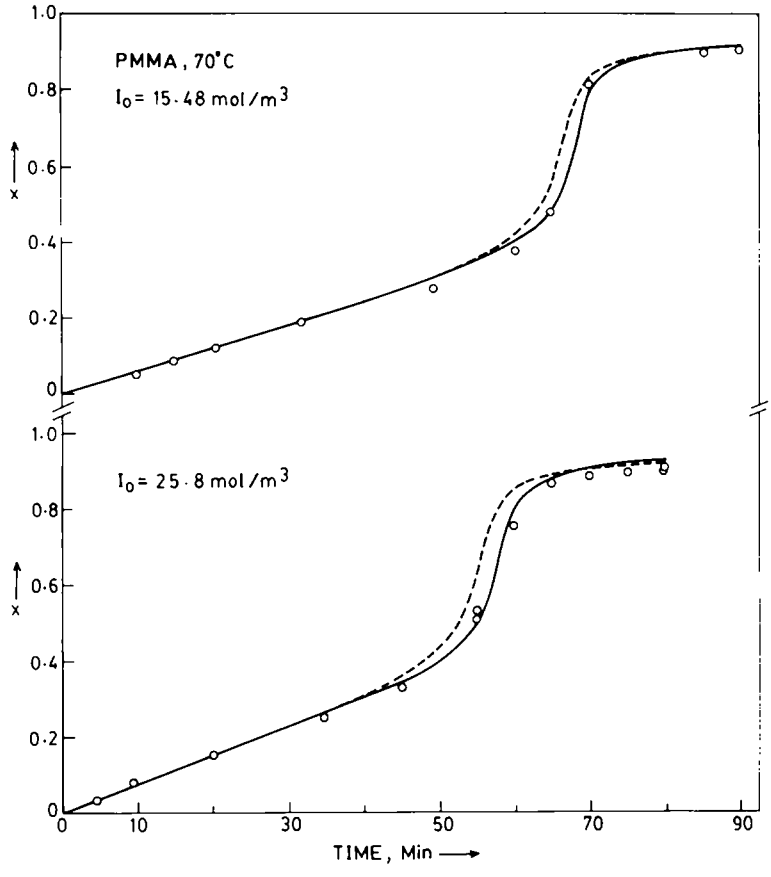

Figure 5 Conversion–time curves for PMMA at 70°C with two initiator loadings. Notation same as in *Figure 3*

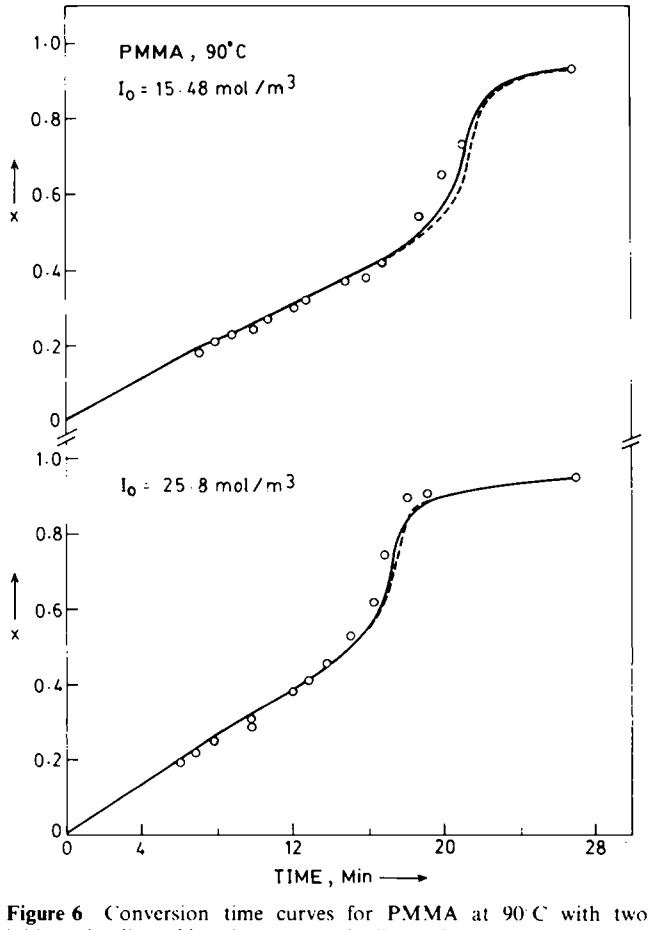

Figure 6 Conversion time curves for PMMA at 90°C with two initiator loadings. Notation same as in *Figure 3*

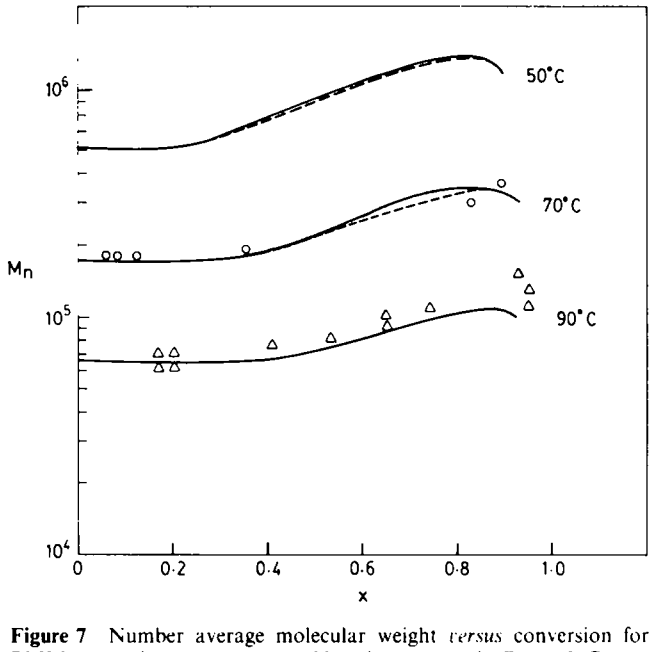

Figure 7 Number average molecular weight *versus* conversion for PMMA at various temperatures. Notation same as in *Figure 3*. Curves are indistinguishable at 90°C. I_0 = 15.48 mol m^{-3}

Ray[27] have suggested that chain transfer to monomer be incorporated in the kinetic scheme of MMA polymerization. We obtained the optimal parameters incorporating this reaction, but found that the agreement of the theoretical predictions with experimental data on the average molecular weights is considerably poorer. We also attempted to obtain optimal values of θ_p, θ_t and A

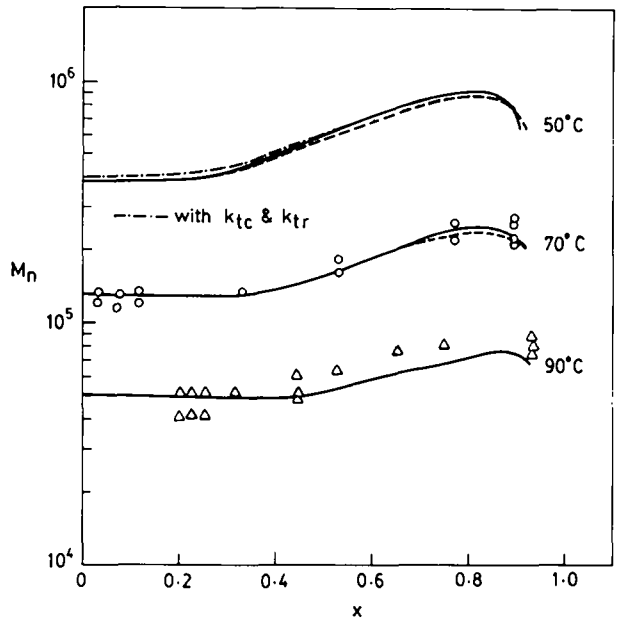

Figure 8 Number average molecular weight *versus* conversion for PMMA at $I_0 = 25.8$ mol m^{-3}. Notation same as in *Figure 7*

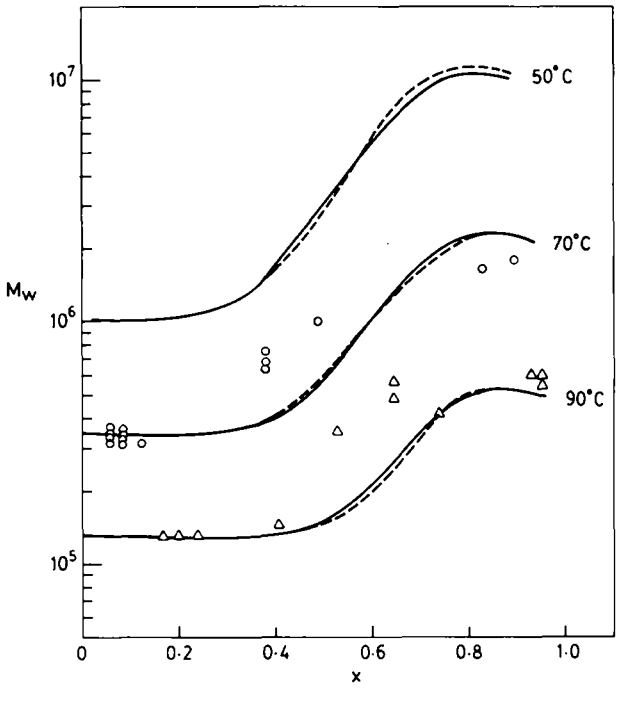

Figure 9 Weight average molecular weight *versus* conversion for PMMA at $I_0 = 15.48$ mol m^{-3}. Notation same as in *Figure 7*

at $T = 50$°C and $I_0 = 25.8$ mol m^{-3} using both chain transfer, as well as termination by combination (with k_{tc}/k_{td} a function of temperature, as used by Baillagou and Soong[15]). It was observed that the optimal values of these parameters at 50°C, with $I_0 = 25.8$ mol m^{-3}, were:

$$\theta_p = 1.8181 \times 10^5 \text{ s}$$
$$\theta_t = 1.3500 \times 10^5 \text{ s} \qquad (6)$$
$$A = 0.12773$$

which are quite close to the set (1.8331×10^5, 1.3552×10^5, 0.12784) given in *Table 9*. The agreement of theoretical predictions with experimental data on monomer conversion improves as seen in *Figure 3*, but

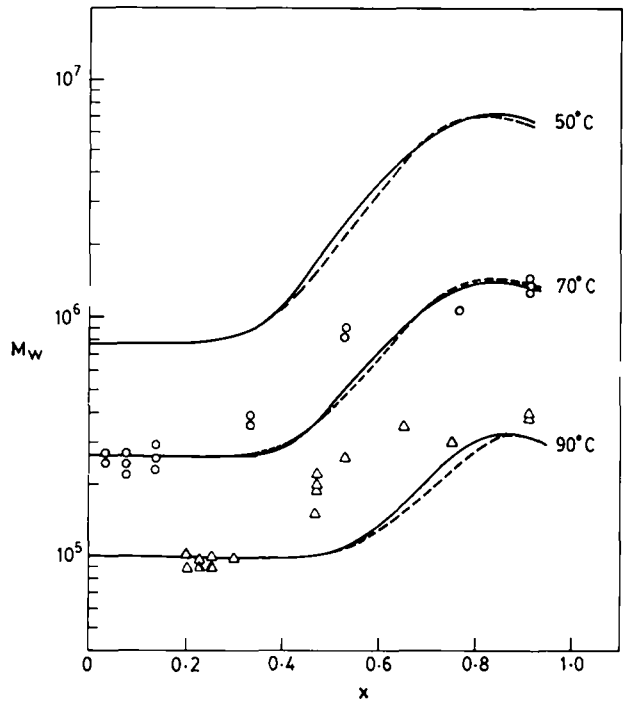

Figure 10 Weight average molecular weight *versus* conversion for PMMA at $I_0 = 25.8$ mol m^{-3}. Notation same as in *Figure 7*

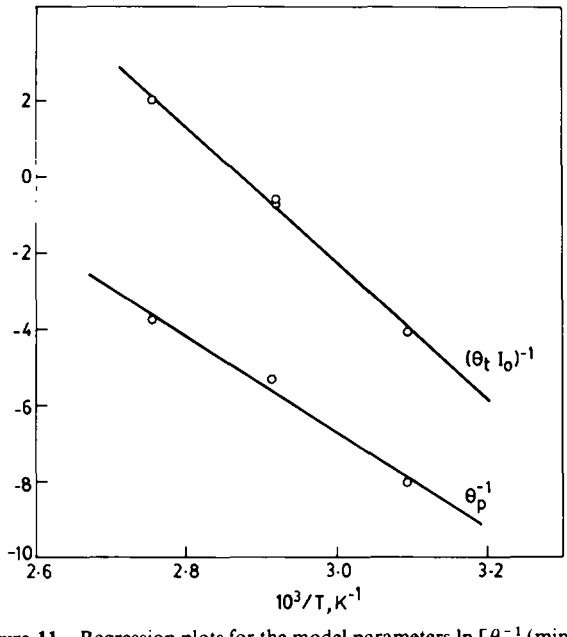

Figure 11 Regression plots for the model parameters ln [θ_p^{-1} (min^{-1})] and ln [$(\theta_t I_0)^{-1}$ (1 mol^{-1} min^{-1})] for PMMA

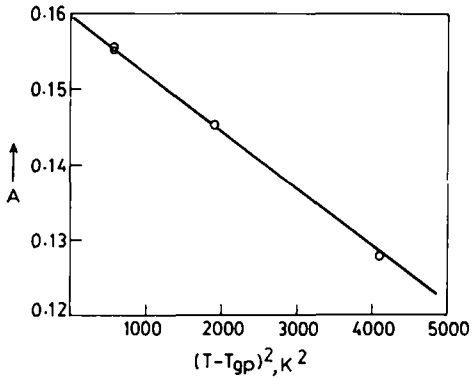

Figure 12 Parameter A (in equation (5c)) *versus* $(T - T_{gp})^2$ for PMMA

higher values of M_n are predicted at low conversions as shown in *Figure 8*. This is similar to what was observed by Achilias and Kiparissides[5] who also incorporated both chain transfer and combination termination. It is difficult at this point to comment on whether these reactions should be incorporated into the kinetic scheme or not, and we did not pursue this approach further, since the parameters in *Table 9* are sufficient to explain current experimental data, and can be used for design, optimization and control of industrial reactors.

As a further application of the optimal parameter estimation technique, we tried to curve-fit some isothermal experimental data on PS, using the model of Chiu *et al.*[1]. A considerable body of data on this system is available in the literature[28–31], not all consistent with each other[30]. We chose to fit the data of Tobolsky[28] since these are available at several temperatures at which thermal initiation of monomer is relatively unimportant. Unfortunately, Tobolsky does not present molecular weight data. In the polymerization of styrene, the termination process takes place through chain transfer as well as by combination (for PMMA, chain transfer is unimportant and termination is by disproportionation). *Table 5* gives the rate constants used. These rate constants were compiled from earlier literature by Duerksen *et al.*[26] and have been used by Kim and Choi[32] to model their bifunctional polymerization of styrene, and have also been reported by Brandrup and Immergut[25] (these, however, differ from values used by Sharma and Soane[12] and Rawlings and Ray[27]). An additional difficulty arises in our study of PS. It is found that on using the values of these rate constants and the initiator efficiency[26] ($f = 0.6$) for the AIBN system, the predictions of the model do not agree with the experimental data, even in the initial region of polymerization where the gel effect is unimportant (a similar disagreement was also observed when we attempted to curve-fit data of Arai and Saito[30] in the low conversion region). So we performed a one variable optimization on Tobolsky's data[28] using our computer package, to obtain an optimal value of the initiator efficiency, f, which can explain the initial range of polymerization. The value of f was found to depend on temperature, and a polynomial fit gave the equation in *Table 5*. A dependence of f on temperature is not unexpected and has been reported by O'Driscoll and Huang[33]. After fitting the value of f using initial conversion data, the Box complex technique is used again this time to obtain the optimal values for the parameters, θ_p, θ_t and A. The data points at 60°C are found to be quite scattered and there is only a single data point in the gel effect region. Hence we performed the optimization study only at 70 and 80°C (even though the 60°C data was also used for obtaining f). The optimal parameters are given in *Table 10*. Again, these parameters are curve-fitted using equation (5) (using only the two points present), and the correlations are shown in *Table 5*. *Figure 13* shows that the agreement between model predictions using these optimal parameters for 70 and 80°C (and correlations for 60°C) and experimental data are quite good. Model predictions for M_n *versus* conversion and M_w *versus* conversion using these parameters have been shown in *Figures 14* and *15*.

It is to be emphasized that our primary motive was to obtain some reasonable correlations for the gel effect for PMMA systems. The polymerization of styrene poses more interesting and challenging optimization problems.

Table 10 Optimal parameters for PS

Temp. (°C)	I_0 (mol m^{-3})	f	$10^{-4}\theta_p(s)$	$10^{-4}\theta_t(s)$	A
60	21.6	0.70	-	-	-
70	21.4	0.764	8.2199	2.8199	0.0814
80	21.2	0.80	5.1925	1.1019	0.08711

$$f = -12.342396 + 9577.287/T(\mathrm{K}) - 1743120.6/[T(\mathrm{K})]^2$$

$$\theta_p(s) = 7.4053 \times 10^{-3} \exp(46.340/RT)$$

$$\theta_t(s) = \frac{1.6886 \times 10^{9}}{I_0} \exp(95.722/RT)$$

$$A = 0.091678 - 1.142 \times 10^{-5}[T(\mathrm{K}) - 373.16]^2$$

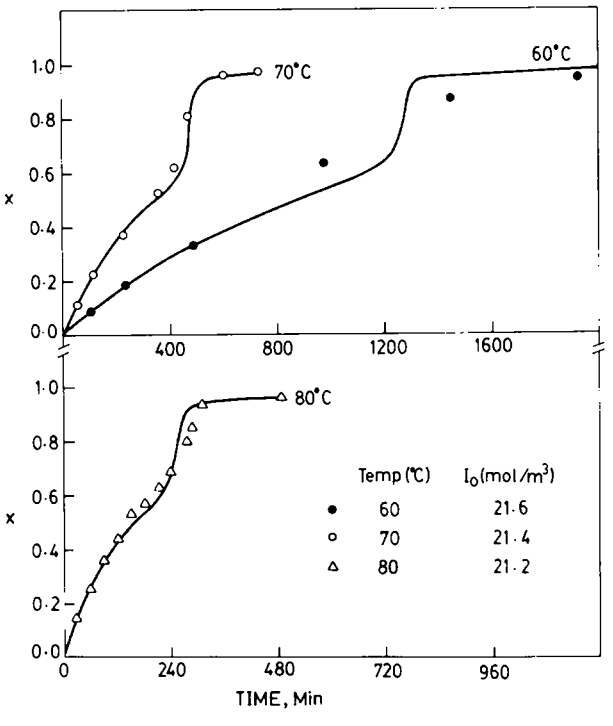

Figure 13 Conversion *versus* time curves for PS at various temperatures. Curves show simulated results using optimal parameters. Data of Tobolsky[28] also shown

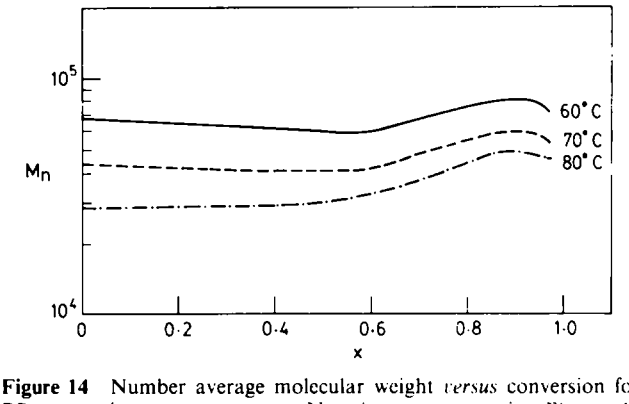

Figure 14 Number average molecular weight *versus* conversion for PS at various temperatures. Notation same as in *Figure 13* (experimental data not available)

For example, it has been reported that f depends on several system characteristics and is even time-dependent[30]. Moreover, thermal initiation effects could be important. All these difficulties can be incorporated in the kinetic equations, and then optimal parameter

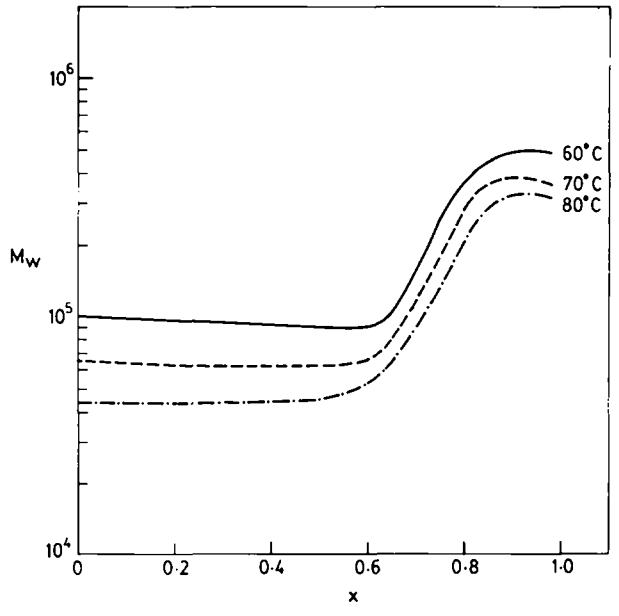

Figure 15 Weight average molecular weight *versus* conversion for PS at various temperatures. Notation same as in *Figure 13*

estimation can be carried out using the approach presented here. The data we have considered in this work for PS has been deliberately selected so that these effects are absent, and we have demonstrated that the technique works well.

CONCLUSIONS

The conversion and molecular weight histories at various temperatures and initiator concentrations, as predicted using the parameters given by Chiu *et al.*[1], are not in good agreement with experimental data on PMMA[16,17], which shows significant gel and glass effects. We have obtained optimal parameters using the Box complex method and have improved the agreement between model predictions and experimental results. The technique is quite general, and as a further illustration of its capabilities, we have estimated the parameters for the free radical polymerization of styrene, using Tobolsky's experimental data[28]. The correlations can be used in the design, simulation, optimization and control of reactors for these systems.

REFERENCES

1 Chiu, W. Y., Carratt, G. M. and Soong, D. S. *Macromolecules* 1983, **16**, 348
2 Trommsdorff, V. E., Kohle, H. and Lagally, P. *Makromol. Chem.* 1947, **1**, 169
3 Schulz, G. V. and Harborth, G. *Makromol. Chem.* 1947, **1**, 106
4 Norrish, R. G. W. and Smith, R. R. *Nature* 1942, **150**, 336
5 Achilias, D. and Kiparissides, C. *J. Appl. Polym. Sci.* 1988, **35**, 1303
6 O'Driscoll, K. F. *Pure Appl. Chem.* 1981, **53**, 617
7 Hamielec, A. E. *Chem. Eng. Commun.* 1983, **24**, 1
8 Friis, N. and Hamielec, A. E. *Am. Chem. Soc. Div. Polym. Chem. Polym. Prepr.* 1975, **16**, 192
9 Ross, R. T. and Laurence, R. L. *AIChE Symp. Ser.* 1976, **160**, 74
10 Cardenas, J. N. and O'Driscoll, K. F. *J. Polym. Sci., Polym. Chem. Edn* 1976, **14**, 883
11 Kapoor, B., Gupta, S. K. and Varma, A. *Polym. Eng. Sci.* 1989, **29**, 1246
12 Sharma, D. K. and Soane, D. S. *Macromolecules* 1988, **21**, 700
13 Tulig, T. J. and Tirrell, M. *Macromolecules* 1981, **14**, 1501
14 Baillagou, P. E. and Soong, D. S. *Chem. Eng. Sci.* 1985, **40**, 75
15 Baillogou, P. E. and Soong, D. S. *Chem. Eng. Sci.* 1985, **40**, 87
16 Marten, F. L. and Hamielec, A. E. *ACS Symp. Ser.* 1979, **104**, 43
17 Balke, S. T. and Hamielec, A. E. *J. Appl. Polym. Sci.* 1973, **17**, 905
18 Louie, B. M., Carratt, G. M. and Soong, D. S. *J. Appl. Polym. Sci.* 1985, **30**, 3985
19 Carratt, G. M., Shervin, C. R. and Soong, D. S. *Polym. Eng. Sci.* 1984, **24**, 442
20 Box, M. *Computer J.* 1965, **8**, 42
21 Kuester, J. L. and Maize, J. H. 'Optimization Techniques with Fortran', 1st Edn, McGraw-Hill, New York, 1973
22 Hock, U. and Schittkowski, K. 'Lecture Notes in Economics and Mathematical Systems', Vol. 187, Springer-Verlag, Berlin, 1981
23 Hui, A. W. T. and Hamielec, A. E. *J. Appl. Polym. Sci.* 1972, **16**, 749
24 Kim, K. J., Liang, W. and Choi, K. *Ind. Eng. Chem. Res.* 1989, **28**, 131
25 Brandrup, J. and Immergut, E. H. (Eds) 'Polymer Handbook', Wiley, New York, 1975
26 Duerksen, J. H., Hamielec, A. E. and Hodgins, J. W. *AIChEJ* 1967, **13**, 1081
27 Rawlings, J. B. and Ray, W. H. *Polym. Eng. Sci.* 1988, **28**, 257
28 Tobolsky, A. V. *J. Am. Chem. Soc.* 1958, **80**, 5927; 1960, **82**, 1277
29 Nishimura, N. *J. Macromol. Sci.* 1966, **2**, 259
30 Arai, K. and Saito, S. *J. Chem. Eng. Jpn* 1976, **9**, 302
31 Schulz, G. V. and Husemann, E. *Z. Phys. Chem.* 1936, **B34**, 187
32 Kim, K. J. and Choi, K. Y. *Chem. Eng. Sci.* 1988, **43**, 965
33 O'Driscoll, K. F. and Huang, J. *Eur. Polym. J.* 1989, **25**, 629

NOMENCLATURE

A, B	Terms in D_0 equation (*Table 2*)
D_n	Dead polymer molecule having n repeating units
E	Error (equation (2))
E_d, E_p	Activation energies of initiation and propagation reactions in the absence of gel and glass effects (kJ mol^{-1})
E_{tc}, E_{td}, E_{tr}	Activation energies of termination by combination, disproportionation and chain transfer in the absence of gel and glass effects (kJ mol^{-1})
$E_{\theta p}$, $E_{\theta t}$	Activation energies for θ_p and θ_t (*Table 2*) (kJ mol^{-1})
f	Initiator efficiency
G_i, H_i	Lower and upper bounds for variable X_i
I	Initiator
I_0	Feed initiator concentration (mol m^{-3})
k_d	Rate constant for initiation (s^{-1})
k_i	Propagation rate constant for primary radical (m^3 mol^{-1} s^{-1})
k_{po}, k_{tco}, k_{tdo}, k_{tro}	Rate constants for propagation, termination by combination and disproportionation and chain transfer in the absence of gel and glass effects (m^3 mol^{-1} s^{-1})
k_d^o, k_{po}^o, k_{tco}^o, k_{tdo}^o, k_{tro}^o	Frequency factors for rate constants of initiation, propagation and termination in the absence of gel and glass effects (m^3 mol^{-1} s^{-1})
M_0	Inlet monomer concentration (mol m^{-3})

M	Monomer concentration at any time (mol m^{-3})
M_n	Number average molecular weight $(\lambda_1 + \mu_1)/(\lambda_0 + \mu_0)$
M_w	Weight average molecular weight $(\lambda_2 + \mu_2)/(\lambda_1 + \mu_1)$
P_n	Growing polymer radical having n repeating units
R*	Primary radical
R	Universal gas constant (kJ mol^{-1} K^{-1})
r_{ij}	Numbers to generate complex
T	Temperature (K)
T_{gp}	Glass transition temperature of polymer (K)
W	Molecular weight of monomer
x	Monomer conversion
ε	Volume contraction factor $[(\rho_m/\rho_p) - 1]$
ε_1	k_1/k_p
μ_k	kth moment of all dead polymer species $\sum_{n=1}^{\infty} (Wn)^k[D_n]; \quad k = 0, 1, 2, \ldots$
ϕ_m	Volume fraction of monomer $[(1 - x)/(1 + \varepsilon x)]$
ρ_m	Density of monomer (kg m^{-3})
ρ_p	Density of polymer (kg m^{-3})
λ_k	kth moment of all polymer radicals $\sum_{n-1}^{\infty} (Wn)^k[P_n] \quad k = 0, 1, 2, \ldots$

Greek letters

$\alpha, \beta, \gamma, \delta$	Parameters in Box complex algorithm
θ_t, θ_p	Characteristic migration times (s)
θ_t^o, θ_p^o	Pre-exponential factors for θ_t and θ_p (s)

Subscripts

o	Inlet value

Superscripts

o	Pre-exponential value